Physics Letters B 754 (2016) 288–293

Contents lists available at ScienceDirect

Physics Letters B

www.elsevier.com/locate/physletb

First direct mass measurements of stored neutron-rich ^{129,130,131}Cd isotopes with FRS-ESR

R. Knöbel [a,*], M. Diwisch [b,1], F. Bosch [a], D. Boutin [a], L. Chen [a,b], C. Dimopoulou [a], A. Dolinskii [a], B. Franczak [a], B. Franzke [a], H. Geissel [a,b], M. Hausmann [c], C. Kozhuharov [a], J. Kurcewicz [a], S.A. Litvinov [a], G. Martinez-Pinedo [d,a], M. Matoš [a], M. Mazzocco [a], G. Münzenberg [a], S. Nakajima [e], C. Nociforo [a], F. Nolden [a], T. Ohtsubo [f], A. Ozawa [g], Z. Patyk [h], W.R. Plaß [a,b], C. Scheidenberger [a,b], J. Stadlmann [a], M. Steck [a], B. Sun [i,a], T. Suzuki [e], P.M. Walker [j], H. Weick [a], M.-R. Wu [d], M. Winkler [a], T. Yamaguchi [e]

[a] GSI Helmholtzzentrum für Schwerionenforschung GmbH, 64291 Darmstadt, Germany
[b] II. Physikalisches Institut, Justus-Liebig-Universität Gießen, 35392 Gießen, Germany
[c] Michigan State University, East Lansing, MI 48824, USA
[d] Physikalisches Institut, Technische Universität Darmstadt, 64289 Darmstadt, Germany
[e] Department of Physics, Saitama University, Saitama 338-8570, Japan
[f] Department of Physics, Niigata University, Niigata 950-2181, Japan
[g] Institute of Physics, University of Tsukuba, Ibaraki 305-8571, Japan
[h] National Centre for Nuclear Research – NCBJ Swierk, Hoża 69, 00-681 Warszawa, Poland
[i] School of Physics and Nuclear Energy Engineering, Beihang University, Beijing 100191, China
[j] Department of Physics, University of Surrey, Guildford, GU2 7XH, United Kingdom

ARTICLE INFO

Article history:
Received 14 July 2015
Received in revised form 18 January 2016
Accepted 21 January 2016
Available online 22 January 2016
Editor: V. Metag

Keywords:
In-flight separation
Storage ring
Isochronous mass spectrometry
Shell closure at $N = 82$
^{129,130,131}Cd isotopes
Mass models

ABSTRACT

A 410 MeV/u ^{238}U projectile beam was used to create cadmium isotopes via abrasion-fission in a beryllium target placed at the entrance of the in-flight separator FRS at GSI. The fission fragments were separated by the FRS and injected into the isochronous storage ring ESR for mass measurements. Isochronous Mass Spectrometry (IMS) was performed under two different experimental conditions, with and without Bρ-tagging at the high-resolution central focal plane of the FRS. In the experiment with Bρ-tagging the magnetic rigidity of the injected fragments was determined with an accuracy of $2 \cdot 10^{-4}$. A new method of data analysis, which uses a correlation matrix for the combined data set from both experiments, has provided experimental mass values of 25 rare isotopes for the first time. The high sensitivity and selectivity of the method have given access to nuclides detected with a rate of a few atoms per week. In this letter we present for the ^{129,130,131}Cd isotopes mass values directly measured for the first time. The experimental mass values of cadmium as well as for tellurium and tin isotopes show a pronounced shell effect towards and at $N = 82$. Shell quenching cannot be deduced from a single new mass value, nor by a better agreement with a theoretical model which explicitly takes into account a quenching feature. This is in agreement with the conclusion from γ-ray spectroscopy and confirms modern shell-model calculations.

1. Introduction

Accurate mass measurements over a range of isotopes reflect details of the evolution of nuclear structure and stability as well as the energy levels and spatial distributions of the bound nucleons [1]. A first microscopic explanation of the observed shell structure and the corresponding magic numbers [2,3] of neutrons and protons, at which the nuclei have larger binding energies, provided the basic understanding of nuclear properties. More recently, the advent and application of radioactive nuclear beam facilities [4] and novel mass spectrometers [5] have enlarged the number of known isotopes with unusual proton-to-neutron ratios and thus revealed novel nuclear properties at the outskirts of the chart of nuclides. Soon it became evident that the nuclear shell structure

* Corresponding author.
E-mail address: R.Knoebel@gsi.de (R. Knöbel).
[1] Part of doctoral thesis at JLU Gießen (2015).

http://dx.doi.org/10.1016/j.physletb.2016.01.039

can change towards the driplines. Shell-gap quenching, complete shell disappearance, or even new magic numbers have been theoretically predicted [6,7] and observed in experiments [8–12].

The best known examples, both theoretically and experimentally, are the $N = 20$ and $N = 28$ "islands of inversion" [11–16] where the gain in correlation energy driven by quadrupole deformation is able to overcome the normal level ordering deduced from the standard spherical mean field. As a result the traditional $N = 20$ and $N = 28$ shell closures disappear. It has also been argued that such a shell quenching would occur for neutron-rich $N = 82$ nuclei. This phenomenon was originally suggested in reference [6], based on Skyrme–Hartree–Fock–Bogoliubov calculations.

Furthermore, nuclear structure properties can strongly influence the synthesis of elements in stars. In this context, it was realized that the occurrence of a discrepant abundance trough in r-process calculations [17] could be cured by using a mass model with a quenched shell gap far from stability [18–20]. The abundance trough around $A \sim 115$ is associated with a 'saddle point behavior' seen in the two-neutron separation energies for $Z \approx 40$ and $N = 75$–82 in several mass models related to a transition from deformed nuclei around $N \sim 75$ to spherical nuclei at $N = 82$ [21]. In mass models with a quenched shell-gap such as the modified extended Thomas–Fermi model (ETFSI-Q) [19] the deformation is greatly reduced and consequently the 'saddle point behavior' in the two-neutron separation energies disappears. However, it should be pointed out that the 'saddle point behavior' and the quenching of the shell gap are not necessarily related [21], because the first one could also be associated with instabilities of mean-field models in regions of shape coexistence, requiring the inclusion of additional correlations [22].

There have been many experimental attempts to provide evidence for the quenching of the shell gap at and near $N = 82$, but most of the information on the shell evolution has been indirect. The present Isochronous Mass Spectrometry (IMS) of the ^{129,130,131}Cd isotopes and the previous Penning trap mass measurements for the tin [23] and tellurium [24] isotopes yield direct information on the shell effects.

2. Experiment and data analysis

Neutron-rich fission fragments created via abrasion-fission were separated in flight for mass measurements. A 410 MeV/u ^{238}U projectile beam was extracted from the synchrotron SIS-18 [25] with an average intensity of $1 \cdot 10^9$/spill and impinged on a 1032 mg/cm^2 beryllium target at the entrance of the fragment separator FRS [26]. The fragments were spatially separated in flight with the FRS by the application of pure magnetic rigidity (Bρ) separation with the standard ion-optical operation mode. The separation mode, without degraders, was enabled by the large mean velocity difference of the projectile fragments and fission products and the restricted angular acceptance of the FRS. Practically this means a suitable $B\rho$-selection with the FRS provided fission-fragment beams without significant contributions of projectile fragments. The ions of interest were injected into the Experimental Storage Ring ESR [27] for mass measurements [28]. The mean velocity of the stored fragments corresponded to the "transition energy" of $\gamma_t = 1.41$. The magnetic fields of the FRS and ESR were set for ^{133,135,136}Sn ions in different runs, i.e., these isotopes were centred at the optical axis.

The ESR was operated in the isochronous mode [29,30] without application of any cooling. This means that the velocity spread of the fragments was determined by the Bρ acceptance of the ion-optical system. In a previous publication [31] we have demonstrated that for IMS experiments, in addition to the revolution time of the stored ions, a magnetic rigidity or velocity measurement is required, because the isochronicity is strictly realized only for a single mass-over-charge (m/q) value.

In principle, this additional measurement is not required for Schottky Mass Spectrometry (SMS) because the relative velocity spread of the different, stored and cooled, ions can be as low as 10^{-7}. Nevertheless, our refined SMS analysis has revealed that an additional influence of the cooler section on the mean velocity causes an observed correlation [32] which has to be taken into account for the final results.

The method of IMS including Bρ-tagging can be illustrated by the simple first-order formula

$$\frac{d(m/q)}{m/q} = \gamma^2 \frac{dT}{T} + \left(1 - \frac{\gamma^2}{{\gamma_t}^2}\right) \frac{d(B\rho)}{B\rho}, \tag{1}$$

where T, γ_t, and γ are the revolution time, the transition energy, and the relativistic Lorentz factor, respectively.

Additional velocity (v) and magnetic-rigidity measurements in FRS-ESR IMS experiments require special methods due to the operation with fast extracted ion bunches characterized by a width of (0.2–0.5) µs. Particle detectors inside the FRS would have severe problems to identify event-by-event the fragments and accurately measure v and $B\rho$. A Bρ-resolution of 10^{-4} or better is required to achieve a mass resolution of about 200 keV for m/q close to ideal isochronicity [33]. In this context, one has to take into account that the FRS transmission is $d(B\rho)/(B\rho) = 2\%$ and the corresponding ESR injection acceptance is more than one order of magnitude less. Therefore, mechanical slits with an opening of ± 0.5 mm placed at the central dispersive focal plane of the FRS were used in a pilot IMS experiment [31,34]. The slits defined in this way the magnetic rigidity (Bρ-tagging) of each injected ion with an accuracy of $2 \cdot 10^{-4}$. Note, that the operation of the new isochronous Rare RI-Ring at RIKEN [35] can implement additional Bρ and v measurements event-by-event, because of the effectively DC beam from the cyclotron accelerator. In the present experiments IMS measurements were performed with and without Bρ-tagging for the same settings of the magnetic fields of the FRS and ESR. The revolution time of the circulating ions in the ring was measured with a time-of-flight (ToF) detector equipped with a thin carbon foil coated with caesium-iodide and two microchannel-plate (MCP) branches [36] placed in a homogeneous magnetic dipole field of about 8.4 mT. The secondary electrons created in the foil were isochronously deflected onto the MCPs to generate timing signals at each turn. The signals were recorded with commercial digital oscilloscopes (Tektronix TDS 6154C, 40 GS/s, 15 GHz; LeCroy LC584AM, 4 GS/s, 1 GHz).

The data sets of the two different experiments, with and without Bρ-tagging, were combined and analysed with a modified correlation-matrix method [37,38]. The separate results of the run with the full Bρ acceptance of the ESR were considered to be unreliable over a large m/q range, see reference [31]. Therefore, we have published up to now only the mass values from the experiment with Bρ-tagging, e.g. [34,39]. The mass range covered in both experiments was almost the same. However, the spectra without Bρ-tagging had much better statistics but were characterized by a factor of more than two larger widths and therefore had much lower resolving power. These aspects and a first comparison of the time spectra have been presented in reference [31]. In the experiment with Bρ-tagging we achieved a mass resolving power of up to 250,000. Without Bρ-tagging the time resolution of the spectra became much worse, especially for m/q values in non-isochronous regions where even non-physical double-peak structures were observed. The much higher mass resolving power in the experiment with Bρ-tagging enabled in this case the proper identification. The combination of both experiments analysed with the modified matrix method yields reliable results even for nuclides with poor

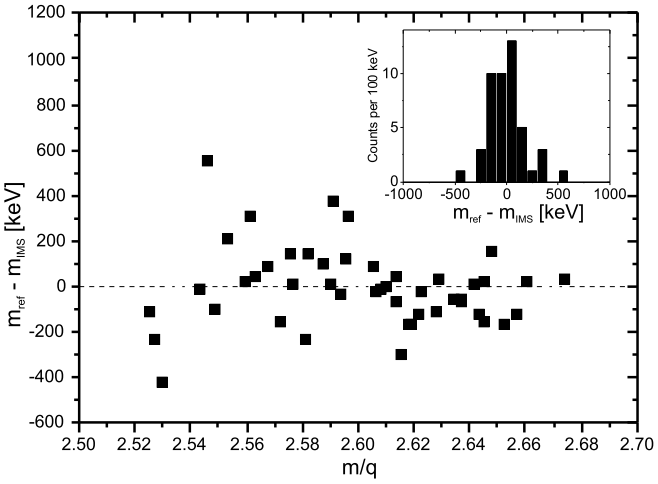

Fig. 1. The systematic error of our mass measurements was determined by reanalysis of each reference mass, i.e., each reference mass is treated sequentially as an unknown species. The distribution of this analysis is depicted as a function of mass-over-charge values and shown in the insert as a projected histogram. Here only the range of the accurately-known reference nuclides is shown. The actual calibration grid is more extended and covers also the cadmium isotopes. Most of the reference masses had good statistics, much larger than 14 recorded ions.

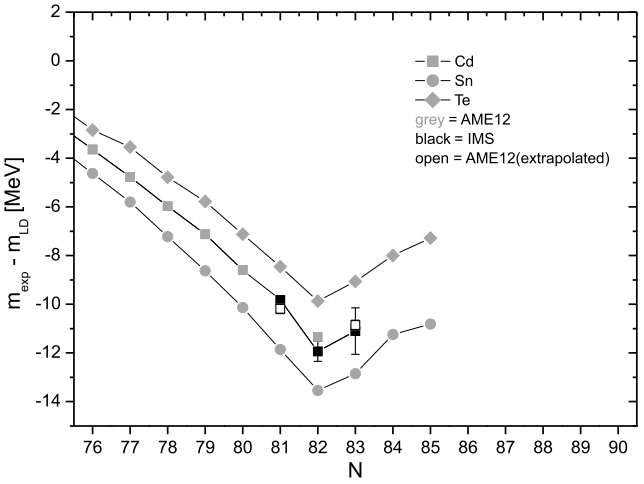

Fig. 2. Difference between the measured mass values and the smooth Weizsäcker formula given by Eq. (3) for the elements tellurium, tin and cadmium. The parameters used in the formula are presented in the text. The data clearly show the extra binding energy due to the contribution of the shell structure for all three elements in this mass region of $N = 82$.

statistics and with a large distance from the accurate reference masses. Most of the stored ions were fully ionized, but a few were recorded in H-like charge states and thus extended the calibration in the neutron-rich region. Note that in the maximum-likelihood method as used in the matrix method [37] all masses were automatically included in the interlinked calibration grid. Furthermore, we used in this work for the first time a variable "s" factor dependent on the measured m/q value, whereas, in reference [37] it was fixed. This variable factor accounts for additional uncertainties of non-isochronous m/q values. The main advantage of the new analysis is that we could include ions with very low rates down to a few events for a single isotope. In this way, we can now present more than 20 new mass values which were not included in previous IMS evaluations of the same experiment [34].

A first check of the reliability of the new data analysis is the determination of the systematic error of the combined experiments. An average of 1600 events per reference mass could be applied in the analysis with the combined data sets. We determined the systematic error by using all accurately-known reference masses and sequentially treating each of these masses as being unknown. The procedure is illustrated by equation 2 and Fig. 1.

$$\sum_{i}^{n} \frac{(m_i - m_i^{ref})^2}{(\sigma_i^{ref})^2 + (\sigma_i^{stat})^2 + (\sigma^{syst})^2} = N_n, \tag{2}$$

where m_i^{ref} are the mass values and σ_i^{ref} the uncertainties of the reference nuclides. σ_i^{stat} are the statistical errors of the measured masses m_i. N_n is the number of reference masses and σ^{syst} the systematic error. In this analysis 47 reference masses have been used [40]. The investigation covers only the m/q range of the accurately-known reference masses. The uncertainty of the reference masses σ_i^{ref} is less than 25 keV, and most of them have an uncertainty well below 10 keV. For m/q > 2.68 no reference masses with the same accuracy were available. The mean value of the projected distribution is 1.29 keV. The deduced systematic error is 172 keV (standard deviation). For most of the new mass values this systematic error is the dominant contribution to the total error which results from the sum of the variances. Different from Penning trap mass measurements, the reference masses are simultaneously measured in the same spectrum together with unknown masses.

In the matrix method the statistical error for each nuclide was calculated by the square root of the diagonal elements of the inverse matrix [37]. In the maximum-likelihood calculation a Gaussian statistical distribution is assumed. However, for very rare nuclides with few recorded events in the whole experiment, a Gaussian description is likely to underestimate the uncertainty. Therefore, we have taken into account an additional systematic error deduced from an observed correlation between the measured uncertainty of the revolution time and the number of turns recorded in the ring. This additional error is quadratically added. It is significant for ions which have made only a few turns in the storage ring. The reason for the observed correlation is probably the influence of the initial phase–space coordinates, e.g., the position and angular coordinates of the injected ions before they reached a closed orbit in the ring. For more than about 14 recorded ions, typically more than three hundred turns have been measured and the contribution of this additional systematic error is no longer significant for the total error.

3. Results and discussion

Fig. 2 shows the difference of the experimental mass values for tellurium, tin and cadmium isotopes and the prediction of the liquid drop model [1,41]. The liquid-drop parameters have been deduced from a fit to the tabulated values of the Atomic Mass Evaluation 2012 (AME12) [42].

The liquid-drop binding energy B_{LD} has the form

$$B_{LD} = b_{vol}A - b_{surf}A^{2/3} - \frac{1}{2}b_{sym}\frac{(N-Z)^2}{A} - \frac{3}{5}\frac{Z^2e^2}{R_c} - \begin{cases} 0 & \text{e–e nuclei} \\ b_{pair}A^{-1/2} & \text{e–o or o–e nuclei} \\ 2\cdot b_{pair}A^{-1/2} & \text{o–o nuclei} \end{cases}, \tag{3}$$

with $R_c = 1.24\ \text{fm} \cdot A^{1/3}$.

The parameters for the Weizsäcker formula from the fit to all measured mass values of reference [42] are: $b_{vol} = 15.747$ MeV, $b_{surf} = 17.603$ MeV, $b_{sym} = 47.494$ MeV, $b_{pair} = 12.822$ MeV.

The strong extra binding energy for the neutron-rich cadmium isotopes is clearly observed. Most of the experimental error bars

Table 1
Measured mass excess values (ME) of cadmium isotopes. The total systematic (σ^{sys}_{total}) and the overall (σ^{total}) errors are tabulated. The common systematic error is 172 keV, see investigations presented in Fig. 1, for all new masses measured. The additional systematic error caused by small numbers of observed revolutions is quadratically added. In addition, the extrapolated (#) values [42] and the ^{130}Cd mass deduced from Q_β-measurement [43] are listed.

Isotope	ME [keV]	σ^{sys}_{total} [keV]	σ^{total} [keV]	ME_{AME12} [keV]	Counts
^{129}Cd	−63145	172	173	−63509(196)#	18
^{130}Cd	−62131	409	411	−61534(164)	5
^{131}Cd	−55583	231	953	−55331(196)#	2

are well within the symbol size. The experimental results in Fig. 2 demonstrate that the tellurium, tin and cadmium isotopes are characterized by almost the same difference of shell corrections towards and at $N = 82$.

For the ^{129,130,131}Cd isotopes the masses have been directly measured for the first time. However, for ^{130}Cd the mass had already been deduced from the measured beta-decay half-live and its Q_β value [43]. Therefore, the mass of ^{130}Cd in the Atomic Mass Evaluation 2012 (AME12) [42] is presently based on this Q_β value. It was concluded in reference [43] that the measured large Q_β-value is an indication of shell quenching because the deduced experimental value was in good agreement with the predictions of the quenched ETFSI-Q mass model [19].

Many experimental [44–46] and theoretical [47,48] investigations of the shell evolution towards and at $N = 82$ were initiated by the conclusions of reference [43]. The new mass values of the present experiment for ^{129,130,131}Cd isotopes follow the measured feature of the tin isotopes and indicate no shell quenching. Thus the comparison between the experimental mass values of tellurium, tin and cadmium demonstrates a strong shell effect for all three elements and clarifies the situation regarding the different statements in the references [44,45,49]. The experimental mass-excess values of ^{129,130,131}Cd nuclei and their errors are presented in Table 1. The mass excess (ME) is defined as the difference between the atomic mass and the corresponding mass number, both expressed in atomic mass units. Our directly measured mass value for ^{130}Cd atoms is about 600 keV lower than the value deduced from Q_β measurements [43]. However, within our large systematic errors both experimental results agree. In principle, in our measurements for ^{129,131}Cd nuclei unresolved isomers could contribute [45,50], whereas for ^{130}Cd nuclei the expected lifetime is too short to interfere in the IMS experiment. Note that in case of isomer contributions, the observed strong shell effect for cadmium isotopes would be even stronger for pure ground-state masses. The nearly equal shell effect for tellurium, tin and cadmium is a striking feature of the present experimental results.

In Fig. 3 the shell evolution is manifested by the one-neutron separation (S_n) energies towards and at $N = 82$. The experimental mass values of this experiment and the values from the AME12 compilation [42] are included. This presentation demonstrates again a strong shell effect towards and at $N = 82$ for tellurium, tin and cadmium isotopes in complete agreement with the characteristics of Fig. 2. Indeed, the experimental observation is that the tellurium, tin and cadmium isotopes are governed by almost the same strong shell gap.

A comparison of the experimental mass values for cadmium and tin isotopes with different theoretical mass models is presented in Fig. 4. The models are based on microscopic–macroscopic descriptions [19,51–53], the Hartree–Fock–Bogoliubov (HFB) theory [54], and the shell-model inspired model of Duflo–Zuker [55].

The comparison of cadmium isotopes demonstrates that the experimental results can deviate from theoretical predictions by more than 1 MeV. Except for ^{130}Cd the models predict too low

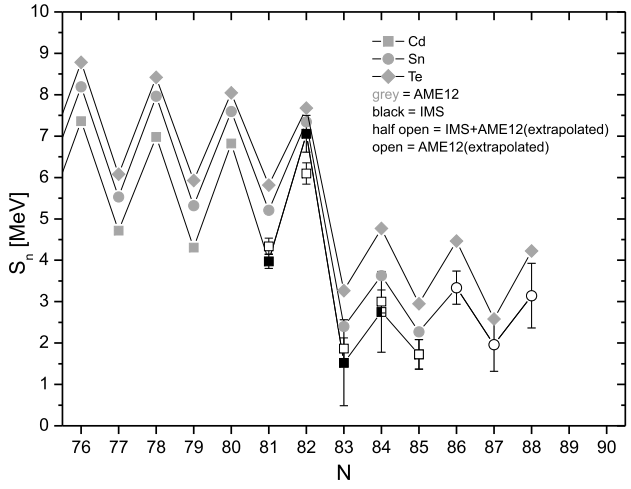

Fig. 3. Experimental one-neutron separation energies (S_n) are shown for cadmium, tin and tellurium isotopes.

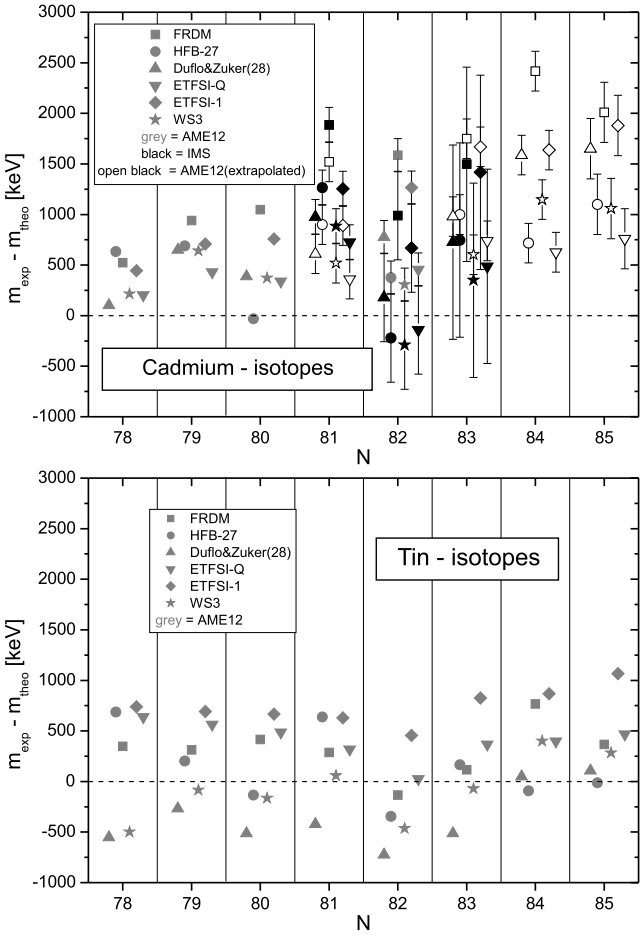

Fig. 4. Comparison of experimental mass values for Cd (upper panel) and Sn (lower panel) isotopes with different theoretical predictions. The N values are grouped in bins in order to facilitate the visual comparison.

mass values (over-binding). For the ^{130}Cd isotope the predictions of the references [19,52,54,55] are quite good and only the predictions from references [51,53] have too small mass values. For $N > 82$, where no experimental data exists, the models widely scatter. From this comparison it is also clearly demonstrated that a better agreement with the quenched ETFSI model cannot be used to declare shell quenching at $N = 82$, because

Table 2
Comparison of measured data with models. The rms deviations are presented for cadmium and tin isotopes compared with the different theoretical models shown in Fig. 4. In this comparison the new IMS values and the tabulated experimental and extrapolated values of AME12 are included. The comparison covers the range of $78 \leq N \leq 85$ as shown in Fig. 4.

	$\sigma_{rms,Cd}$ [keV]	$\sigma_{rms,Sn}$ [keV]
FRDM [51]	1537	392
HFB-27 [54]	775	370
DZ28 [55]	958	450
ETFSI-Q [19]	512	444
ETFSI-1 [53]	1200	762
WS3 [52]	709	306

mass models without this quenching agree equally well with the experimental data. The comparison with tin isotopes shows different features, it reflects that the masses for tin isotopes have been experimentally well known for a long time, for example, the mass value of the ^{132}Sn isotope was already quite well known ($\pm$80 keV) in 1983. A consequence is that the corresponding differences among the models are much smaller. However, the systematic difference of the ETFSI-Q and ETFSI models is also clearly seen for the tin isotopes at $N = 82$. It is noteworthy that for ^{132}Sn and ^{130}Cd isotopes the agreement of experimental mass values and the ETFSI-Q model is excellent.

The global predictive power of the different models can be quantitatively characterized by the σ_{rms} values. They are listed in Table 2 for tin and cadmium isotopes in the range of $78 \leq N \leq 85$ as selected in the Fig. 4. It is clearly observed in this comparison that the σ_{rms} values are up to a factor 3 larger for the Cd isotopes.

During the refereeing process of the present Letter, new experimental mass values for the $^{129-131}$Cd isotopes were published [57]. The published results have an uncertainty of less than 100 keV. The experimental mass values for ^{129}Cd and ^{131}Cd isotopes agree within the error bars of the present IMS experiment, but the values for ^{130}Cd differ by 1013 keV, which is outside of the standard deviation listed in Table 1. The ISOLTRAP value is also 416 keV higher than the value deduced from beta-decay spectroscopy [43]. Possible reasons that the trap mass value is higher than the values of both other experiments could be an influence of an unknown isomeric state or unknown systematic errors. A conclusion is that the mass for ^{130}Cd should be independently remeasured at an other facility such as TITAN-TRIUMF [58] or RIBF-RIKEN [59].

From the present experiments we can state that our new mass values for cadmium isotopes are not consistent with a quenching of the $N = 82$ shell gap closure to ^{132}Sn as claimed before by several publications [43,56]. However, a disappearance of the shell gap for lighter isotones cannot be ruled out. Therefore, it is necessary to have experimental access to isotones with $Z \leq 42$, for which the differences between models become substantial.

4. Summary and outlook

IMS experiments have been performed with and without Bρ-tagging at the FRS-ESR facilities at GSI. A new method of data analysis using the correlation matrix for the combined data of both types of experiment provided 25 new mass values in the range of Ge to Ce ($A = 86$–154) even for isotopes measured with a rate of a few atoms per week [33]. The latter condition demonstrates the high sensitivity and selectivity of the experimental method. A detailed description of the analysis and the new mass values will be presented in a forthcoming publication. In this letter we have presented the masses of the ^{129,130,131}Cd isotopes which have been directly measured for the first time. A goal of this letter was to present the evolution of the shell gap of Cd isotopes compared with tellurium and tin isotopes towards and at $N = 82$. The Cd results show a pronounced shell effect, which is consistent with modern shell-model calculations. The experimental values for the shell corrections are roughly the same for the tin, tellurium and cadmium isotopes.

The goal of future IMS experiments will be to measure the masses of elements with lower proton numbers ($40 \leq Z < 48$) towards and at the $N = 82$ shell closure. The mass values of these elements will be decisive for the determination of possible shell quenching as proposed in several theoretical models. However, experimentally this interesting region can only be accessed by the next generation of exotic nuclear beam facilities [59–62].

Acknowledgements

We would like to thank Yu.A. Litvinov and J.S. Winfield for fruitful discussions. This work was supported by the German Federal Ministry of Education and Research (BMBF) numbers 06GI9115I and 06DA7047I, the Helmholtz Association (HGF) through the Nuclear Astrophysics Virtual Institute (VH-VI-417), the Helmholtz International Center for FAIR (HIC for FAIR) within the framework of the LOEWE program launched by the State of Hesse, and the UK Science and Technology Facilities Council.

References

[1] A. Bohr, B. Mottelson, Nuclear Structure Vols. I, II, World Scientific, 1998.
[2] M. Goeppert-Mayer, Phys. Rev. 74 (1948) 235;
M. Goeppert-Mayer, Phys. Rev. 75 (1949) 1969.
[3] O. Haxel, J.H.D. Jensen, H.E. Suess, Phys. Rev. 75 (1949) 1766.
[4] H. Geissel, et al., in: R. Stock (Ed.), Encyclopedia of Nuclear Physics and Its Applications, Wiley-VCH, 2013, p. 161.
[5] Int. J. Mass Spectrom. 349–350 (2013) 1-276, edited by Yu.A. Litvinov, K. Blaum.
[6] J. Dobaczewski, et al., Phys. Rev. Lett. 72 (1994) 981.
[7] T. Otsuka, et al., Phys. Rev. Lett. 87 (2001) 082502.
[8] C. Thibault, et al., Phys. Rev. C 12 (1975) 644.
[9] A. Ozawa, et al., Phys. Rev. Lett. 84 (1994) 5493.
[10] R. Kanungo, Phys. Scr. T 152 (2013) 014002.
[11] D. Guillemaud-Mueller, et al., Nucl. Phys. A 426 (1984) 37.
[12] T. Motobayashi, et al., Phys. Lett. B 346 (1995) 9.
[13] B. Bastin, et al., Phys. Rev. Lett. 99 (2007) 022503.
[14] B.A. Brown, Prog. Part. Nucl. Phys. 47 (2001) 517.
[15] E. Caurier, et al., Rev. Mod. Phys. 77 (2005) 427.
[16] E. Caurier, F. Nowacki, A. Poves, Phys. Rev. C 90 (2014) 014302.
[17] K.-L. Kratz, et al., Astrophys. J. 403 (1993) 216.
[18] B. Chen, et al., Phys. Lett. B 355 (1995) 37.
[19] J.M. Pearson, R.C. Nayak, S. Goriely, Phys. Lett. B 387 (1996) 455.
[20] B. Pfeiffer, K.-L. Kratz, F.K. Thielemann, Z. Phys. A 357 (1997) 235.
[21] H. Grawe, K. Langanke, G. Martínez-Pinedo, Rep. Prog. Phys. 70 (2007) 1525.
[22] T.R. Rodríguez, A. Arzhanov, G. Martínez-Pinedo, Phys. Rev. C 91 (2015) 044315.
[23] M. Dworschak, et al., Phys. Rev. Lett. 100 (2008) 072501.
[24] J. Hakala, et al., Phys. Rev. Lett. 109 (2012) 032501.
[25] K. Blasche, B. Franczak, in: Proc.: 3rd Eur. Part. Acc. Conf, Berlin, 1992, p. 9.
[26] H. Geissel, et al., Nucl. Instrum. Methods, Sect. B 70 (1992) 286.
[27] B. Franzke, Nucl. Instrum. Methods, Sect. B 24–25 (1987) 18.
[28] B. Franzke, H. Geissel, G. Münzenberg, Mass Spectrom. Rev. 27 (5) (2008) 428.
[29] M. Hausmann, et al., Nucl. Instrum. Methods, Sect. A 446 (2000) 569.
[30] A. Dolinskii, et al., Nucl. Instrum. Methods, Sect. A 574 (2007) 207.
[31] H. Geissel, et al., Hyperfine Interact. 173 (2006) 49.
[32] L. Chen, et al., Nucl. Phys. A 882 (2012) 71.
[33] M. Diwisch, Doctoral thesis, Justus-Liebig University Gießen, 2015.
[34] B. Sun, et al., Nucl. Phys. A 812 (2008) 1.
[35] A. Ozawa, T. Uesaka, M. Wakasugi, Prog. Theor. Exp. Phys. (2012) 03C009.
[36] J. Trötscher, et al., Nucl. Instrum. Methods Phys. Res., Sect. B 70 (1992) 455.
[37] T. Radon, et al., Nucl. Phys. A 677 (2000) 75.
[38] Yu.A. Litvinov, et al., Nucl. Phys. A 734 (2004) 473.
[39] B. Sun, et al., Eur. Phys. J. A 31 (2007) 393.
[40] JYFLTRAP, http://research.jyu.fi/igisol/JYFLTRAP_masses/nrich.html.
[41] C.F. von Weizsäcker, Z. Phys. 96 (1935) 431.
[42] G. Audi, et al., Chin. Phys. C 36 (2012) 1287.
[43] I. Dillmann, et al., Phys. Rev. Lett. 91 (2003) 162503.

[44] A. Jungclaus, et al., Phys. Rev. Lett. 99 (2007) 132501.
[45] J. Taprogge, et al., Phys. Rev. Lett. 112 (2014) 132501.
[46] G. Lorusso, et al., Phys. Rev. Lett. 114 (2015) 192501.
[47] T.R. Rodríguez, J.L. Egido, A. Jungclaus, Phys. Lett. B 668 (2008) 410.
[48] D.T. Yordanov, et al., Phys. Rev. Lett. 110 (2013) 192501.
[49] M. Gorska, et al., Phys. Lett. B 672 (2009) 313.
[50] J. Taprogge, et al., Phys. Lett. B 738 (2014) 223.
[51] P. Möller, et al., At. Data Nucl. Data Tables 59 (1995) 185.
[52] N. Wang, M. Liu, J. Phys. 420 (2013) 012057.
[53] Y. Aboussir, et al., At. Data Nucl. Data Tables 61 (1995) 127.
[54] S. Goriely, N. Chamel, J.M. Pearson, Phys. Rev. C 88 (2013) 061302(R), http://www-astro.ulb.ac.be/bruslib/nucdata/hfb27-dat.
[55] J. Duflo, A.P. Zuker, Phys. Rev. C 52 (1995) 23.
[56] T. Kautzsch, et al., Eur. Phys. J. A 9 (2000) 201.
[57] D. Atanasov, et al., Phys. Rev. Lett. 115 (2015) 23201.
[58] J. Dilling, et al., Nucl. Instrum. Methods, Sect. B 204 (2003) 492.
[59] T. Kubo, Nucl. Instrum. Methods, Sect. B 204 (2003) 97.
[60] H. Geissel, et al., Nucl. Instrum. Methods, Sect. B 204 (2003) 71.
[61] M. Hausmann, et al., Nucl. Instrum. Methods, Sect. B 317 (2013) 349.
[62] Y. Blumenfeld, et al., Int. J. Mod. Phys. E 18 (2009) 1960.